



## OPEN Mathematical modelling of the role of Langerhans cells in the dynamics of HPV infection

Fahad Al Basir<sup>1</sup>, Konstantin B. Blyuss<sup>2</sup>, Aeshah A. Raezah<sup>3</sup>, Bootan Rahman<sup>4</sup> & Hebatallah J. Alsakaji<sup>5</sup>✉

Cervical cancer is the second most frequent gynaecological malignancy in the world. Human papillomavirus (HPV) infection is the primary etiologic agent of cervical cancer. However, HPV alone is not sufficient for tumor progression. The clinical display of HPV infection also depends on the host's immune status. Both innate and adaptive immunity recognize and fight foreign pathogens inside the body, but sometimes they prove ineffective against HPV. HPV has several mechanisms for evading the immune system. After infection, HPV multiplies in keratinocytes, which are distant from immune centers and have a naturally short lifespan. The naturally short life cycle of the keratinocyte removes the need for the virus to destroy the cells, which would trigger inflammation and immune response. In addition, HPV downregulates the expression of interferon genes. Despite viral immune evasion, the immune system effectively resists most HPV infections and mounts strong localized cell mediated immune responses. Despite significant progress in observations and clinical practice, many aspects of the complex interactions between HPV and the human immune system remain not fully understood. Langerhans cells (LCs) are known to play a critical role in producing innate and adaptive cellular immune responses against HPV infection. In this paper, we propose and analyze a mathematical model of HPV infection with particular focus on the role of Langerhans cells in facilitating immune response, as well as on the treatment of HPV infection by induction of the appropriate virus-specific immune responses in patients. We determine equilibria of the model, analyse their stability, and derive the basic reproduction number. Sensitivity analysis is performed to investigate the effects of individual parameters on system dynamics. We explore the impulsive therapy for controlling HPV infection, and discuss how these findings may be helpful in development of immunotherapy against HPV infection.

**Keywords** HPV infection, Langerhans cells, Stability analysis, Numerical simulations, Basic reproduction number, Impulsive control approach

Human papillomavirus (HPV) is widely known to be a cause of intraepithelial cervical neoplasia (CIN) and cervical cancer. Worldwide, cervical cancer is both the fourth-most common cause of cancer, and the fourth-most common cause of death from cancer in women<sup>1,2</sup>. In 2022, an estimated 660,000 cases of cervical cancer occurred worldwide, with 350,000 deaths<sup>2</sup>, which is about 8% of the total cases and total deaths from cancer<sup>3</sup>. By 2030, the global burden of cervical cancer is expected to increase to over 700,000 cases and over 400,000 deaths per year, with over 95% of these deaths taking place in low- and middle-income countries<sup>4</sup>. "Cervical cancer" is the term for a malignant neoplasm arising from cells originating in the tissues of the cervix, part of the female reproductive system. Over 95% of cervical cancers are caused by an infection with the human papilloma virus (HPV)<sup>4</sup>. Among over 130 HPV types, around 40 HPV types can infect the genital areas of men and women, including the skin of the penis, vulva and anus, cervix and rectum<sup>5</sup>. Among these, HPV16 and 18 types are considered to be of particularly high risk and progression to cervical cancer<sup>6</sup>.

Human papilloma viruses (HPV) are small DNA viruses with a circular genome of approximately 8000bp that infect the basal cell layer of epidermis. Their genome is functionally divided into three regions. The first is a non-coding upstream regulatory region (URR). The second is an early region, encrypting the early viral proteins E6, E7, E8, E1, E2, E4 and E5, and the third is a late region, encrypting L1 and L2 proteins, which are components

<sup>1</sup>Department of Mathematics, Asansol Girls' College, Asansol-4, Asansol, West Bengal 713304, India. <sup>2</sup>Department of Mathematics, University of Sussex, Falmer, Brighton BN1 9QH, UK. <sup>3</sup>Department of Mathematics, Faculty of Science, King Khalid University, 62529 Abha, Saudi Arabia. <sup>4</sup>Mathematics Unit, School of Science and Engineering, University of Kurdistan Hewlêr (UKH), Erbil, Iraq. <sup>5</sup>Department of Mathematical Sciences, College of Science, UAE University, 15551 Al Ain, UAE. ✉email: heba.sakaji@uaeu.ac.ae

of the viral capsid. E1 protein facilitates viral replication using the host replication machinery. The E5, E6, and E7 proteins are considered to be associated with virus immune evasion. The E6 and E7 gene products deregulate the host cytotoxic lymphocyte growth cycle by binding and inactivating two tumor suppressor proteins: the tumor suppressor protein (p53) and the retinoblastoma gene product (pRb)<sup>7</sup>. Consequently, the normal activities of p53 that manage arrest, apoptosis, and DNA repair of G1 are abolished<sup>8,9</sup>. Inactivation of the p53 and pRb proteins can lead to an increased proliferation and genomic instability, resulting in accumulation of DNA damage and leading to transformed cancerous cells<sup>10</sup>. Prior to development of cervical cancer, there are several stages of dysplasia that correspond to different proportions of basal epithelial cells being occupied by abnormal cells<sup>11</sup>. The progression from initial infection to cervical cancer is typically slow, often over a period of 20 or more years. During that time, the disease develops through a precancerous stage that can be detected through a regular cytological examination of the cervix with a Pap test. If the screening confirms an abnormality, additional testing and treatment can usually eliminate the disease.

The immune system plays an important role in clearing most of HPV infections, but some infections cannot be eliminated and persist for several years, becoming an additional risk factor<sup>12</sup>. Once an antigen is detected by the body, there are two types of immune responses the body can use to defend itself<sup>13</sup>. The first line of defense is the immediate response called the innate immune system, which is non-specific to the antigen. The second, long-lasting line of defense is the adaptive immune system<sup>13</sup>. This type of immune response is antigen-specific and has a memory of antigens it has come across before, but it takes longer to act, because it takes some time for immune system to recognize foreign antigens and mount responses in the form of antigen-specific antibodies and cytotoxic T cells.

During the early stages of an HPV infection, the innate immune response of the host is the first line of defense against infection. Dendritic cells (DCs), Langerhans cells (LCs), natural killer (NK), natural killer T (NKT) cells and keratinocytes, among others, plays an important role in promoting a good adaptive immune response against HPV infection. Most of these cell types can promote a cytokine-mediated pro-inflammatory process that links the innate and the adaptive immune responses. Furthermore, NK cells are able to directly eliminate HPV-infected cells<sup>14</sup>. Langerhans cells (LC) are the primary type of antigen-presenting dendritic cells that reside in epidermis<sup>15</sup>. These cell play an essential role in triggering adaptive immune response against viral antigens that can be found in the epidermis<sup>16</sup>. However, HPV can evade the immune response, mainly through the action of E6 and E7 proteins<sup>17,18</sup>.

One of the first attempts to mathematically model cancer immunotherapy was made by Kirschner and Panetta<sup>19</sup>. They developed a system of equations describing external inflow of both IL-2 and cultured immune cells, and analysed immunotherapy based on the use of IL-2 together with adoptive cellular immunotherapy (ACI). de Boer and Hogeweg<sup>20</sup> studied a mathematical model of cellular immune response to tumors and showed that initially small doses of antigens lead to tumor dormancy. Kuznetsov et al.<sup>21,22</sup> developed models of immunogenic tumors that exhibit oscillatory growth patterns when the tumor stays very small for a relatively long period of time, and subsequently grows to become dangerously large. A model proposed by Dingli and Michor<sup>23</sup> includes cancer stem cells and several potential forms of treatment. Freedman and Belostotski<sup>24,25</sup> developed model for radiation treatment based on a system of two differential equations for healthy and cancerous cells. That work analyzed four different methods of describing how the radiation treatment was administered—as a constant, proportional to the number of cancer cells, proportional to the ratio of cancer cells to healthy cells, and periodically. The effects of periodic radiation have also been studied by Liu et al.<sup>26</sup>. Isaeva and Osipov<sup>27</sup> analyzed a model that includes combined effects of chemo- and immunotherapy. They showed tumor-immune dynamics under the influence of both immunotherapy with IL-2 and IFN- $\alpha$  and chemotherapy. Very recently, Rajan et al.<sup>28</sup> have performed sensitivity analysis for this model to estimate the parameter values and identified key parameters that influence transmission.

In this paper, we consider a model of immune response to HPV infection that includes Langerhans cells, acting as sentinels, and cytotoxic lymphocytes able to eliminate infected cells. Besides establishing conditions for existence and stability of the steady states, we also utilize an impulsive control approach to find appropriate dosing interval that allows to control infection through treatment.

The rest of paper is arranged as follows. In Sect. “[The mathematical model](#)” we present necessary biological background and formulate the mathematical model. Well-posedness and equilibria of the model are discussed in Sect. “[Model well-posedness and steady states](#)”. Section “[Basic reproduction number and stability of equilibria](#)” established basic reproduction number of the model and contains results on stability of equilibria, as well as sensitivity analysis. Section “[Impulsive control approach](#)” is devoted to impulsive control approach for possible treatment of HPV infection. Numerical bifurcation analyses and simulations are performed in Sect. “[Numerical bifurcation analyses and simulation](#)”. The paper concludes in Sect. “[Discussion and conclusion](#)” with a discussion of results and future research.

## The mathematical model

Following<sup>29,30</sup>, we consider HPV infection starting when free virions, whose population will be denoted by  $V(t)$ , infect healthy basal cells at rate  $\beta$ . With the total population of all epithelial cells assumed to be constant  $N$ , the number of basal epithelial cells that are thus infected will be denoted by  $E_I(t)$ , with the remaining  $(N - E_I)$  cells being uninfected cells that can potentially be infected in the future. Infection is assumed to be density-dependent, with constant  $\sigma$  representing the concentration of uninfected cells at half-maximum growth. Once infected, the cells  $E_I$  traverse up through the epithelial column and transform into transit-amplifying infected cells  $E_T$  cells that reside in supra-basal (mid-layer) of the epithelium<sup>31,32</sup>. We will denote by  $\mu$  the rate of conversion from  $E_I$  to  $E_T$  cells, and it represents the rate of expression of HPV oncogenes E6 and E7, once the cells become infected. Higher levels of expression of these oncogenes by  $E_T$  cells and location of these cells

in the supra-basal layer allows these cells to additionally self-replicate at a rate  $r\mu$ . For simplicity, we assume that both types of HPV-infected cells,  $E_I$  and  $E_T$ , die at the same rate  $d$ . With HPV being a non-lytic virus, new virions are released from infected cells through bursting of infected cells. Since both  $E_I$  and  $E_T$  express oncogenes and thus produce new virions, we will assume that the rate of production of new virions is, therefore, equal to  $kd$  and the same for both types of infected cells. Virions are assumed to be cleared at a constant rate  $d_v$  that implicitly captures antibody response.

An important role in controlling HPV infection is played by cellular immunity and, in particular, by cytotoxic T cell lymphocytes (CTLs)<sup>17,18,33</sup>. To better understand the dynamics of CTL response, we include in the model a population of intra-epithelial Langerhans cells (LCs), which are antigen-presenting cells that are critical in T-cell priming in response to viral infections of the skin. HPV infection is directly associated with a reduction in the number of LCs in infected epidermis<sup>34</sup>. At the same time, LCs phagocytose vaginal epithelial cells undergoing apoptosis, as was demonstrated in the murine model<sup>35</sup>. We will assume LCs, to be denoted  $L(t)$ , are produced at a constant growth rate  $\lambda$  and die at rate  $d_l$ . The number of LCs can increase through recruitment of other LCs in the presence of infected cells  $E_T$ , expressing high concentrations of E6 and E7 oncogenes<sup>36,37</sup>, and we assume this to happen at rate  $\eta$ . On the other hand, HPV is known to be capable both of immune evasion, and it can also reduce antigen presentation by downregulating NF- $\kappa$ B signalling in HPV-infected cells, and by inhibiting keratinocyte-derived CCL20 expression, which, in turn, affects LCs and limits their capacity to stimulate CD8+ T cells<sup>38–40</sup>. In the model this is represented by a reduction of the growth in LCs with a half-maximum growth constant  $\theta$  and with the amount of free virus  $V$ .

Finally, we assume that HPV-specific CTLs, denoted  $Z(t)$ , are produced at a constant growth rate  $s$  and cleared at rate  $d_z$ , and their population also grows proportionally to the number of LCs and CTLs at rate  $\alpha$ . CTLs kills infected cells at rate  $a$ , which is assumed to be the same for both types of infected cells,  $E_I$  and  $E_T$ .

Based on the above assumptions, we have the following model for dynamics of HPV infection

$$\begin{aligned}\frac{dE_I}{dt} &= \frac{\beta V(N - E_I)}{\sigma + (N - E_I)} - \mu E_I - dE_I - aE_I Z = f_1(x), \\ \frac{dE_T}{dt} &= \mu E_I + r\mu E_T - dE_T - aE_T Z = f_2(x), \\ \frac{dV}{dt} &= kd(E_I + E_T) - d_v V = f_3(x), \\ \frac{dL}{dt} &= \lambda + \frac{\eta E_T L}{\theta + V} - d_l L = f_4(x), \\ \frac{dZ}{dt} &= s + \alpha Z L - d_z Z = f_5(x),\end{aligned}\quad (1)$$

where  $x = (E_I, E_T, V, L, Z)$ , with biologically-relevant initial conditions

$$E_I(0) \geq 0, E_T(0) \geq 0, V(0) \geq 0, L(0) \geq 0, Z(0) \geq 0. \quad (2)$$

### Model well-posedness and steady states

Since the right-hand sides  $f_i(x)$  of the model (1) are smooth functions of its variables, standard theory of differential equations guarantees the existence of a unique solution for the system (1) with initial conditions (2)<sup>41,42</sup>. Before proceeding with analysis of the model, we now establish its well-posedness in terms of non-negativity and boundedness of solutions.

Let us introduce auxiliary quantities

$$B_1 = \frac{\mu N}{d - r\mu}, \quad B_2 = \frac{\lambda}{d_l - \eta B_1}, \quad B_3 = \frac{s}{d_z - \alpha B_2}, \quad (3)$$

and assume that the following conditions hold

$$d > r\mu, \quad d_l > \eta B_1, \quad d_z > \alpha B_2. \quad (4)$$

Biologically, the first of these conditions implies that the death rate of epithelial cells should exceed the growth rate of self-proliferating cells, which is true for experimentally observed values of parameters as used in earlier papers<sup>29,30</sup>. The second and third conditions prevent unbounded growth of Langerhan cells and the CTLs, respectively.

Now, we have the following result.

**Proposition 1** *All solutions of system (1) with initial conditions (2) remain non-negative and bounded in  $\mathcal{D}$  for all  $t \geq 0$ , where*

$$\mathcal{D} = \left\{ (E_I, E_T, V, L, Z) \in \mathbb{R}_+^5 : 0 \leq E_I \leq N, 0 \leq E_T \leq B_1, \right. \\ \left. 0 \leq V \leq \frac{kd(N + B_1)}{d_v}, 0 \leq L \leq B_2, 0 \leq Z \leq B_3 \right\}. \quad (5)$$

*Proof* Considering the equation for  $E_I$ , let  $t_I > 0$  be the first time when  $E_I(t_I) = 0$ , with other variables being non-negative as per initial conditions, i.e.

$$E_T(t) \geq 0, V(t) \geq 0, L(t) \geq 0, Z(t) \geq 0 \text{ for } t \in [0, t_I].$$

The first equation of the system (1) shows that at this moment of time,

$$\frac{dE_I}{dt}(t_I) = \frac{\beta V(t_I)N(t_I)}{\sigma + N} \geq 0,$$

suggesting that  $E_I$  cannot decrease below zero. Similarly, if  $t_L > 0$  is the first time when  $L(t_L) = 0$ , with other variables remaining non-negative, we immediately recognise that since

$$\frac{dL}{dt}(t_L) = \lambda > 0,$$

from this moment of time  $L$  will increase and, hence, it also can never become negative. Using the same argument sequentially for other variables shows that for non-negative initial conditions, all variables will remain non-negative for all  $t \geq 0$ .

From the first equation of system (1), we have

$$\frac{dE_I}{dt} = \frac{\beta V(N - E_I)}{\sigma + (N - E_I)} - \mu E_I - dE_I - aE_I Z \leq \frac{\beta V(N - E_I)}{\sigma + (N - E_I)} = \beta V \left( 1 - \frac{\sigma}{\sigma + N - E_I} \right).$$

If  $E_I$  exceeds  $N$ , the last bracket becomes negative, and  $E_I$  decreases, thus showing that  $E_I(t) \leq N$  for all  $t \geq 0$ . From the second equation, using  $E_I \leq N$ , we have

$$\frac{dE_T}{dt} = \mu E_I + r\mu E_T - dE_T - aE_T Z \leq \mu E_I + r\mu E_T - dE_T \leq \mu N - (d - r\mu)E_T. \tag{6}$$

In light of the condition  $d > r\mu$  given in (4), we then have

$$0 \leq E_T \leq \frac{\mu N}{d - r\mu} = B_1.$$

In a similar way, we can obtain a bound on  $V(t)$  as

$$0 \leq V \leq \frac{kd(N + B_1)}{d_v}.$$

The fourth equation of system (1) can be rewritten as

$$\frac{dL}{dt} = \lambda + \frac{\eta E_T L}{\theta + V} - d_l L \leq \lambda + \eta B_1 L - d_l L = \lambda - (d_l - \eta B_1)L.$$

which shows that

$$0 \leq L \leq \frac{\lambda}{d_l - \eta B_1} = B_2.$$

Finally, from the last equation of system (1), we get

$$\frac{dZ}{dt} = s + \alpha Z L - d_z Z \leq s + \alpha B_2 Z - d_z Z = s - (d_z - \alpha B_2)Z, \tag{7}$$

implying

$$0 \leq Z \leq \frac{s}{d_z - \alpha B_2} = B_3.$$

From this analysis, we conclude that the region  $\mathcal{D}$  is positively invariant, with all solutions of the system (1) with initial conditions in  $\mathcal{D}$  remaining within this region for all  $t \geq 0$ .  $\square$

The system (1) can have two equilibria, namely,

- i. the disease-free equilibrium  $E_0 \left( 0, 0, 0, \frac{\lambda}{d_l}, \frac{sd_l}{d_z d_l - \alpha \lambda} \right)$ ,
- ii. the chronic equilibrium  $E^* (E_I^*, E_T^*, V^*, L^*, Z^*)$ ,

where

$$\begin{aligned}
 E_I^* &= \frac{(d_l L^* - \lambda)\theta d_v (d + aZ^* - r\mu)}{H^*}, \\
 E_T^* &= \frac{(d_l L^* - \lambda)\mu\theta d_v}{H^*}, \\
 V^* &= \frac{kdE_I^* (d + aZ^* + \mu - r\mu)}{d_v (d + aZ^* - \mu r)}, \\
 L^* &= \frac{d_z Z^* - s}{\alpha^* Z^*},
 \end{aligned}$$

with

$$H^* = kd(\lambda - d_l)(\mu + d + aZ^* - \mu) + \mu\eta d_v L^*,$$

and  $Z^*$  is the positive root of the following equation:

$$\Phi(Z) = \beta V(N - E_I) - [\sigma + (N - E_I)](\mu + d + aZ)E_I = C_0 Z^5 + C_1 Z^4 + C_2 Z^3 + C_3 Z^2 + C_4 Z + C_5 = 0, \quad (8)$$

where the coefficient of  $Z^5$  is

$$\begin{aligned}
 C_0 &= N\alpha^3 dd_l^2 d_v d_z^2 k + N\alpha^3 \alpha^2 dd_v k \lambda^2 + \alpha^3 d_l^2 d_v^2 d_z^2 \theta + \alpha^3 \alpha^2 d_v^2 \lambda^2 \theta + \alpha^3 \alpha^2 dd_v k \lambda^2 \sigma \\
 &\quad + \alpha^3 dd_l^2 d_v d_z^2 k \sigma - 2\alpha^3 \alpha dd_l d_v d_z k \lambda \sigma - 2N\alpha^3 \alpha dd_l d_v d_z k \lambda - 2\alpha^3 \alpha d_l d_v d_z \lambda \theta.
 \end{aligned}$$

and the constant term  $C_5$  is given by

$$\begin{aligned}
 C_5 &= -3d^2 d_l^2 d_v k \mu^2 r s^2 \sigma - Ndd_l^2 d_v k \mu^3 r s^2 - 2Nd^3 d_l^2 d_v k \mu r s^2 + \beta dd_l^2 d_v k \mu^2 r s^2 \theta + 2\beta d^2 d_l^2 d_v k \mu r s^2 \theta - dd_l^2 d_v k \mu^3 r s^2 \sigma \\
 &\quad + dd_l^2 d_v k \mu^3 r^2 s^2 \sigma + d^3 d_l^2 d_v^2 s^2 \theta - N\beta d^4 d_l^2 k^2 s^2 + d^2 d_l^2 d_v^2 \mu s^2 \theta + d_l^2 d_v^2 \mu^3 r^2 s^2 \theta + Nd^4 d_l^2 d_v k s^2 + d^4 d_l^2 d_v k s^2 \sigma \\
 &\quad - N\beta d^2 d_l^2 k^2 \mu^2 s^2 - Ndd_l d_v^2 \eta \mu^2 s^2 - Nd^2 d_l d_v^2 \eta \mu s^2 + 2Nd^3 d_l^2 d_v k \mu s^2 + Nd_l d_v^2 \eta \mu^3 r s^2 - \beta d^3 d_l^2 d_v k s^2 \theta - dd_l d_v^2 \eta \mu^2 s^2 \sigma \\
 &\quad - d^2 d_l d_v^2 \eta \mu s^2 \sigma + 2d^3 d_l^2 d_v k \mu s^2 \sigma - 2N\beta d^3 d_l^2 k^2 \mu s^2 + d_l d_v^2 \eta \mu^3 r s^2 \sigma + Nd^2 d_l^2 d_v k \mu^2 s^2 - 2dd_l^2 d_v^2 \mu^2 r s^2 \theta - 2d^2 d_l^2 d_v^2 \mu r s^2 \theta \\
 &\quad + 2N\beta d^2 d_l^2 k^2 \mu^2 r s^2 + N\alpha^2 d^2 d_v k \lambda^2 \mu^2 z^2 + Nd^2 d_l^2 d_v k \mu^2 r^2 s^2 - N\beta dd_l d_v \eta k \mu^2 r s^2 + N\beta dd_l d_v \eta k \mu^2 s^2 + N\beta d^2 d_l d_v \eta k \mu s^2 \\
 &\quad + 2N\beta d^3 d_l^2 k^2 \mu r s^2 - 3Nd^2 d_l^2 d_v k \mu^2 r s^2 + Ndd_l^2 d_v k \mu^3 r^2 s^2 - N\beta d^2 d_l^2 k^2 \mu^2 r^2 s^2 + dd_l d_v^2 \eta \mu^2 r s^2 \sigma + d^2 d_l^2 d_v k \mu^2 r^2 s^2 \sigma \\
 &\quad + Ndd_l d_v^2 \eta \mu^2 r s^2 - 2d^3 d_l^2 d_v k \mu r s^2 \sigma + d^2 d_l^2 d_v k \mu^2 s^2 \sigma - \beta d^2 d_l^2 d_v k \mu s^2 \theta - \beta dd_l^2 d_v k \mu^2 r^2 s^2 \theta.
 \end{aligned}$$

Since, Eq. (8) is quintic, therefore, at least one of its roots is real. For the values of parameters from Table 1, and for all other parameter ranges explored in later sections, the value of the coefficient  $C_5$  is negative, while  $C_0$  is positive, suggesting the existence of a positive real root of Eq. (8).

Biologically, the disease-free steady state  $E_0$  describes a situation, where the immune system is able to successfully clear the infection, while the chronic state  $E^*$ , when it exists, is a steady state, where immune response fails, and the infection continues to persist at some steady level. While the disease-free steady state  $E_0$  is feasible for any parameter values, the chronic steady state  $E^*$  only exists in some part of the parameter space.

Parameters	Description	Value
$N$	Total epithelial cells	$10^5$
$\sigma$	Half-saturation constant	$10^6$
$k$	HPV burst size	1000 virions/cell
$\alpha$	Proliferation rate of CTLs	$0.001 \text{ day}^{-1}$
$\beta$	Infection rate of uninfected cells	$0.0067 \text{ day}^{-1}$
$d_v$	Decay rate of free virions	$0.05 \text{ day}^{-1}$
$r$	Self-division rate of infected cells	0.1
$d$	Death rate of epithelial cells	$0.048 \text{ day}^{-1}$
$a$	Killing rate of infected cells by CTLs	$0.01 \text{ day}^{-1}$
$s$	Recruitment rate of CTLs	$0-2 \text{ cells ml}^{-1} \text{ day}^{-1}$
$\lambda$	LC recruitment rate	$0-1 \text{ cells ml}^{-1} \text{ day}^{-1}$
$\eta$	Proliferation rate of LCs	$2.5 \times 10^{-6} \text{ day}^{-1}$
$\mu$	Rate of oncogene expression	$0.25 \text{ day}^{-1}$
$d_l$	Clearance rate of LCs	$0.25 \text{ day}^{-1}$
$d_z$	Clearance rate of CTLs	$0.13 \text{ day}^{-1}$
$\theta$	Half-saturation constant	$10^4$

**Table 1.** Values of the model parameters<sup>29,30,53–56</sup>.

As we have noted earlier, the Eq. (8) has a positive root  $Z^*$  for all values of parameters we explored, but this does not guarantee that the chronic steady state is biologically feasible with all its components being positive.

Figure 1 establishes the existence of chronic equilibrium.

### Basic reproduction number and stability of equilibria

In the context of modelling the spread of infectious diseases, one of the fundamental concepts is that of *basic reproduction number*  $\mathcal{R}_0$ <sup>43-45</sup>. This number quantifies an average number of secondary infections produced by a single infected individual in an otherwise entirely susceptible population. Subject to some generic assumptions, if the basic reproduction number exceeds one, there would be an outbreak of infectious disease, and if it is less than one, the disease would die out. The magnitude of the the basic reproduction number is used epidemiologically to quantify and compare severity/virulence of infections, with larger values of  $\mathcal{R}_0$  signifying higher transmissibility.

Later, the concept of the basic reproduction number has also been used in the analysis of within-host mathematical models of immune response to viral infection<sup>46-49</sup>. In those models,  $\mathcal{R}_0 > 1$  describes a situation, where after a certain number of host cells are infected with a virus, there would be further growth in the number of infected cells due to the spread of virions to as yet uninfected cells, whereas for  $\mathcal{R}_0 < 1$ , initial infection would be successfully cleared by the immune system without spreading to other cells.

To compute the basic reproduction number  $\mathcal{R}_0$  for our model, we use the next-generation matrix method<sup>50,51</sup>. To this end, we consider the next generation matrix  $G$  as comprised of two parts, namely,  $F$  and  $V$ . The vector containing all terms associated with transmission from infected to non-infected classes is represented by  $\mathcal{F}$ , and similarly, the vector of transitions between infected classes is represented by  $\mathcal{V}$ . The Jacobian matrices for these two vectors  $\mathcal{F}$  and  $\mathcal{V}$  are denoted by  $F$  and  $V$ , respectively. The  $i^{th}$  row and  $j^{th}$  column elements of the matrix  $F$  are  $F_{ij}$ , with  $F_{ij} = \frac{\partial \mathcal{F}_i}{\partial x_j}$ , where  $\mathcal{F}_i$  is the  $i^{th}$  component of  $\mathcal{F}$ , and  $x_j$  is the  $j^{th}$  variable of the vector of infected classes. Similarly,  $V_{ij}$  is the entry of matrix  $V$ 's  $i^{th}$  row and  $j^{th}$  column, with  $V_{ij} = \frac{\partial \mathcal{V}_i}{\partial x_j}$ . Here,  $x_j$  is the  $j^{th}$  variable of the vector of infected classes, and  $\mathcal{V}_i$  is the  $i^{th}$  component of  $\mathcal{V}$ .

For the model (1), we find vectors  $\mathcal{F}$  and  $\mathcal{V}$  as

$$\mathcal{F} = \begin{pmatrix} \frac{\beta V(N-E_I)}{\sigma+(N-E_I)} \\ 0 \\ 0 \end{pmatrix}, \quad \mathcal{V} = \begin{pmatrix} \mu E_I + dE_I + aE_I Z \\ -r\mu E_T - r\mu E_T + dE_T + aE_T Z \\ d_v V \end{pmatrix}$$

which, when evaluated at the disease-free equilibrium  $E_0$ , gives

$$F(E_0) = \begin{bmatrix} 0 & 0 & \frac{\beta N}{N+\sigma} \\ 0 & 0 & 0 \\ 0 & 0 & 0 \end{bmatrix}$$

$$V(E_0) = \begin{bmatrix} \mu + d + a\bar{Z} & 0 & 0 \\ -\mu & -r\mu + d + a\bar{Z} & 0 \\ -kd & -kd & d_v \end{bmatrix},$$

where  $\bar{Z} = \frac{sd_I}{d_I d_z - \alpha \lambda}$ . The basic reproduction number  $\mathcal{R}_0$  can now be determined as the dominant eigenvalue of the matrix  $G = FV^{-1}$ <sup>50,51</sup>. Thus,

$$\mathcal{R}_0 = \frac{\beta kdN(\mu + d + a\bar{Z} - \mu r)}{(N + \sigma)d_v(d + \mu + a\bar{Z})(d + a\bar{Z} - \mu r)}. \tag{9}$$

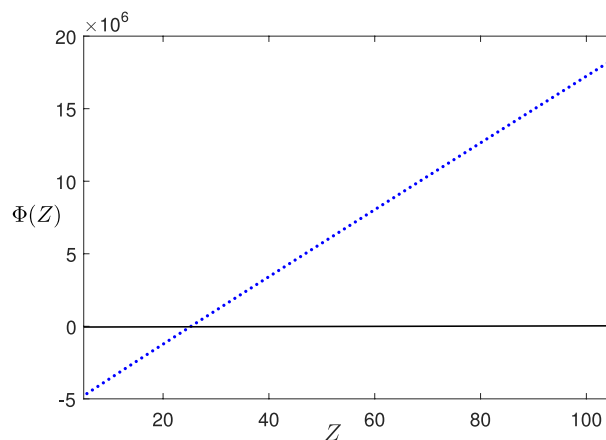


Fig. 1. Polynomial  $\Phi(Z)$  as given by (8) with parameter values from Table 1.

As is common in epidemiological/immunological models, the basic reproduction number  $\mathcal{R}_0$  increases with infection rate  $\beta$  and the total number of epithelial cells  $N$  that can potentially be infected, and decreases with increasing rate of viral clearance  $d_v$ . The value of  $\mathcal{R}_0 < 1$  describes a situation, where an initial infection is successfully cleared by the immune system and does not result in subsequent infection of other uninfected cells. In contrast, for  $\mathcal{R}_0 > 1$ , immune system is not capable to clear the virus before it infects other cells, resulting in the ongoing infection.

Now we use this basic reproduction number to obtain stability conditions for the disease-free steady state.

### Stability of disease-free equilibrium

The Jacobian matrix at the disease-free equilibrium,  $E_0$  is obtained as

$$J_{E_0}(0, 0, 0, \bar{L}, \bar{Z}) = \begin{bmatrix} a_{11} & 0 & a_{13} & 0 & 0 \\ a_{21} & a_{22} & 0 & 0 & 0 \\ a_{31} & a_{32} & a_{33} & 0 & 0 \\ 0 & \frac{\eta\bar{L}}{\theta} & 0 & -d_l & 0 \\ 0 & 0 & 0 & \alpha\bar{Z} & \alpha\bar{L} - d_z \end{bmatrix},$$

where  $\bar{Z} = sd_l/(d_z d_l - \alpha\lambda)$ ,  $\bar{L} = \lambda/d_l$ , and we also have  $a_{13} = \beta N/(\sigma + N)$ ,  $a_{21} = \mu$ ,  $a_{31} = a_{32} = kd$ , and  $a_{33} = -d_v$ ,  $a_{11} = -\mu - d - a\bar{Z} < 0$  and  $a_{22} = r\mu - d - a\bar{Z} < 0$  due to invariance (5).

Two eigenvalues of the Jacobian are  $\rho_1 = -d_l < 0$ ,  $\rho_2 = \alpha\bar{L} - d_z$ . Using the condition (4) we can show that  $\rho_2 < 0$ . The remaining three eigenvalues  $\rho_{3,4,5}$  satisfy the cubic equation

$$\rho^3 + \gamma_1\rho^2 + \gamma_2\rho + \gamma_3 = 0. \tag{10}$$

where,

$$\begin{aligned} \gamma_1 &= -(a_{11} + a_{22} + a_{33}), \quad \gamma_2 = a_{22}a_{33} + a_{11}a_{22} - a_{13}a_{31} + a_{11}a_{33}, \\ \gamma_3 &= -a_{13}a_{21}a_{31} + a_{13}a_{22}a_{31} - a_{11}a_{22}a_{33}. \end{aligned} \tag{11}$$

Using the Routh–Hurwitz conditions, we obtain that the roots of (10) have negative real parts if the following conditions are satisfied:

$$\begin{aligned} (i) \quad & \gamma_1 > 0, \quad \gamma_3 > 0, \\ (ii) \quad & \gamma_1\gamma_2 - \gamma_3 > 0. \end{aligned} \tag{12}$$

After a straightforward calculations and using (5), we conclude that  $\gamma_1 = \mu + d + 2a\bar{Z} + d_v + (d - r\mu) > 0$ . If we rewrite  $\mathcal{R}_0$  as

$$\mathcal{R}_0 = \frac{\beta kdN(\mu + d + a\bar{Z} - \mu r)}{(N + \sigma)d_v(d + \mu + a\bar{Z})(d + a\bar{Z} - \mu r)} = \frac{a_{13}a_{31}(a_{21} - a_{22})}{-a_{11}a_{22}a_{33}},$$

we obtain

$$\begin{aligned} \gamma_3 &= -a_{13}a_{21}a_{31} + a_{13}a_{22}a_{31} - a_{11}a_{22}a_{33} \\ &= -a_{11}a_{22}a_{33} \left( 1 - \frac{a_{13}a_{31}(a_{21} - a_{22})}{-a_{11}a_{22}a_{33}} \right) \\ &= (-a_{11})a_{22}a_{33}(1 - \mathcal{R}_0). \end{aligned}$$

Hence, for  $\mathcal{R}_0 < 1$ , we have  $\gamma_3 > 0$ . Similarly,

$$\begin{aligned} \gamma_1\gamma_2 - \gamma_3 &= (\mu + d + a\bar{Z} + d + a\bar{Z} - r\mu + d_v) \left\{ d_v(d + a\bar{Z} - r\mu) + (\mu + d + a\bar{Z})d_v \right. \\ &\quad \left. + (\mu + d + a\bar{Z})(d + a\bar{Z} - r\mu) - kd\frac{\beta N}{\sigma + N} \right\} - \left\{ (\mu + d + a\bar{Z})(d + a\bar{Z} - r\mu)d_v \right. \\ &\quad \left. - \frac{kd\beta N(d + \mu + a\bar{Z} - r\mu)}{\sigma + N} \right\} \\ &> 2(\mu + d + a\bar{Z})(d + a\bar{Z} - r\mu)d_v - \frac{kd\beta N(d + \mu + a\bar{Z} - r\mu)}{\sigma + N} + \frac{kd\beta N}{\sigma + N}(\mu + d - r\mu - d_v) + d_v^2(\mu + 2d + 2a\bar{Z} - \mu r) \\ &> d_v(\mu + d + a\bar{Z})(d + a\bar{Z} - r\mu)(1 - \mathcal{R}_0) + d_v \left[ d_v[(\mu + d + a\bar{Z}) + (d + a\bar{Z} - \mu r)] - \frac{kd\beta N}{\sigma + N} \right] \\ &> [(\mu + d + a\bar{Z})(d + a\bar{Z} - r\mu)d_v] (1 - \mathcal{R}_0) + \frac{d_v^2(\mu + d + a\bar{Z})(d + a\bar{Z} - r\mu)}{(d + \mu + a\bar{Z} - r\mu)} [1 - \mathcal{R}_0] \\ &> 0, \text{ if } \mathcal{R}_0 < 1, \end{aligned}$$

where we have used the fact that  $d > r\mu$  as given by (4).

Following the above discussion, we have the following result for the stability of disease-free equilibrium,  $E_0$ .

**Theorem 1** *The disease-free equilibrium  $E_0$  is stable if  $\mathcal{R}_0 < 1$  and unstable when  $\mathcal{R}_0 > 1$ .*

### Stability of chronic equilibrium

As discussed in the previous section, while the value of  $Z^*$  as determined by the real positive root of Eq. (8) is always positive, this is not automatically true for other components of the chronic steady state  $E^*$ . Numerical simulations suggests that this steady state is indeed biologically feasible with all of its components being non-negative for  $\mathcal{R}_0 \geq 1$ . To analyse stability of the chronic equilibrium  $E^*(E_I^*, E_T^*, V^*, L^*, Z^*)$ , we evaluate the Jacobian at this steady state as

$$J_{E^*} = [J_{ij}] = \begin{bmatrix} J_{11} & 0 & \frac{\beta(N-E_I^*)}{\sigma+N-E_I^*} & 0 & -aE_I \\ \mu & r\mu - d - aZ^* & 0 & 0 & -aE_T^* \\ kd & kd & -d_v & 0 & 0 \\ 0 & J_{42} & J_{43} & J_{44} & -\eta \\ 0 & 0 & 0 & \alpha Z^* & \alpha L^* - d_z \end{bmatrix}$$

where,

$$J_{11} = -\mu - d - aZ^* - \frac{\beta\sigma V^*}{(\sigma + N - E_I^*)^2},$$

$$J_{42} = \frac{\eta L^*}{(\theta + V^*)}, \quad J_{43} = -\frac{\eta E_T^* L^*}{(\theta + V^*)^2}, \quad J_{44} = \frac{\eta E_T^*}{(\theta + V^*)} - d_l.$$

The characteristic equation at  $E^*$  has the form

$$\xi^5 + A_1\xi^4 + A_2\xi^3 + A_3\xi^2 + A_4\xi + A_5 = 0, \quad (13)$$

with

$$\begin{aligned} A_1 &= -(J_{11} + J_{22} + J_{33} + J_{44} + J_{55}), \\ A_2 &= J_{11}(J_{22} + J_{33} + J_{44}) - J_{13}J_{31} + J_{22}(J_{33} + J_{44}) + J_{33}(J_{44} + J_{55}) + J_{55}(J_{11} + J_{22}) + J_{44}J_{55}, \\ A_3 &= J_{13}J_{31}(J_{44} - J_{21}) + J_{22}(J_{13}J_{31} - J_{11}J_{33}) - J_{22}J_{44}(J_{11} + J_{55}) - J_{33}J_{44}(J_{11} + J_{22}) - J_{25}J_{42}J_{54} - J_{11}J_{44}J_{55} \\ &\quad - J_{11}J_{22}J_{55} + J_{13}J_{31}J_{55} - J_{11}J_{33}J_{55} - J_{22}J_{33}J_{55} - J_{33}J_{44}J_{55}, \\ A_4 &= J_{13}J_{44}(J_{21}J_{31} - J_{22}J_{31}) + J_{11}J_{22}J_{33}J_{44} - J_{15}J_{21}J_{42}J_{54} + J_{25}J_{33}J_{42}J_{54} - J_{15}J_{31}J_{43}J_{54} - J_{25}J_{31}J_{43}J_{54} \\ &\quad + J_{11}J_{25}J_{42}J_{54} + J_{13}J_{21}J_{31}J_{55} - J_{13}J_{22}J_{31}J_{55} + J_{11}J_{22}J_{33}J_{55} \\ &\quad + J_{11}J_{22}J_{44}J_{55} - J_{13}J_{31}J_{44}J_{55} + J_{11}J_{33}J_{44}J_{55} + J_{22}J_{33}J_{44}J_{55}, \\ A_5 &= (J_{13}J_{25}J_{31} + J_{15}J_{21}J_{33})J_{42}J_{54} - J_{11}J_{25}J_{33}J_{42}J_{54} - J_{15}J_{43}J_{54}(J_{21}J_{31} + J_{22}J_{31}) + J_{11}J_{25}J_{31}J_{43}J_{54} \\ &\quad - J_{22}J_{31}) - J_{13}J_{21}J_{31}J_{44}J_{55} + J_{22}J_{44}J_{55}(J_{13}J_{31} - J_{11}J_{33}). \end{aligned}$$

According to Routh–Hurwitz criteria, the characteristic equation (13) has roots with negative real parts if the following conditions hold

$$\begin{aligned} (i) \quad & A_5 > 0, \quad A_1A_2 - A_3 > 0, \\ (ii) \quad & A_3(A_1A_2 - A_3) - A_1(A_1A_4 - A_5) > 0, \\ (iii) \quad & (A_1A_4 - A_5) \cdot (A_1A_2A_3 - A_3^2 - A_1^2A_4) - A_5(A_1A_2 - A_3)^2 - A_1A_5^2 > 0. \end{aligned} \quad (14)$$

**Theorem 2** *The chronic equilibrium is asymptotically stable when the conditions in (14) are satisfied, and unstable when any of these conditions is violated.*

### Sensitivity analysis

Besides direct effect of parameters on stability of the disease-free and chronic steady states, we can use the methodology proposed<sup>52</sup> to explore sensitivity of model solutions with respect to changes in parameters. The sensitivity functions with respect to the killing rate  $a$  of infected cells by the CTLs are defined as

$$\begin{aligned} S_{E_{I_a}}(t) &= \frac{\partial}{\partial a} E_I(t), \quad S_{E_{T_a}}(t) = \frac{\partial}{\partial a} E_T(t), \quad S_{V_a}(t) = \frac{\partial}{\partial a} V(t), \\ S_{L_a}(t) &= \frac{\partial}{\partial a} L(t), \quad S_{Z_a}(t) = \frac{\partial}{\partial a} Z(t). \end{aligned} \quad (15)$$

These sensitivity functions satisfy the following system of ODEs

$$\begin{aligned}
 \frac{dS_{E_{I_a}}}{dt} &= \beta S_{V_a} [E_T + VS_{E_{T_a}} + 2V + L + S_{L_a}V + Z + VS_{Z_a}] \cdot \frac{\sigma + (N - E_I)(1 - V)}{(\sigma + (N - E_I))^2} \\
 &\quad - S_{E_{I_a}}(\mu + d + aZ) - E_I(aS_{Z_a} + Z), \\
 \frac{dS_{E_{T_a}}}{dt} &= \mu S_{E_{I_a}} + (r\mu - d)S_{E_{T_a}} - E_T Z - a(S_{E_{T_a}}Z + S_{Z_a}E_T), \\
 \frac{dS_{V_a}}{dt} &= kd(S_{E_{I_a}} + S_{E_{T_a}}) - d_v S_{V_a}, \\
 \frac{dL_a}{dt} &= -d_l S_{L_a} + \frac{\eta(LS_{E_{T_a}} + E_T S_{L_a})(\theta + V) - \eta S_{V_a} E_T L}{(\theta + V)^2}, \\
 \frac{dS_{Z_a}}{dt} &= \alpha(S_{Z_a}L + ZS_{L_a}) - d_z S_{Z_a}.
 \end{aligned}
 \tag{16}$$

To understand how the sensitivity functions (15) evolve in time, we need to solve the system (16) together with the original system (1). In a similar way, we can study sensitivity of the model with respect to other parameters.

### Impulsive control approach

While preventive HPV vaccines play a fundamental role in controlling the spread of HPV and prevention of HPV-associated lesions and cancers, they cannot help with treatment of already established HPV infection. Although there are currently no specific treatments against HPV, several different clinical approaches are being explored. One of those approaches is the so-called therapeutic vaccines, which instead of generating neutralizing antibodies instead contribute to cell-mediated immunity. HPV-encoded E6 and E7 oncoproteins that are consistently expressed in HPV-associated cancers and precursor lesions play crucial roles in the generation and maintenance of HPV-associated disease, which makes them an ideal target for therapeutic vaccines. Various forms of therapeutic HPV vaccines targeting HPV E6/E7 antigens have been tested in preclinical models and clinical trials<sup>57,58</sup>.

Another possible approach to treatment of HPV is that of adoptive cell immunotherapy, where CTLs targeting E6/E7 antigens are isolated and then re-infused to patients, thus boosting their ability to eliminate HPV-infected cells<sup>59-61</sup>. While still being at the stage of clinical trials, this methodology is very promising from the perspective of providing patient-specific targeted treatment.

Below is a modified model of HPV dynamics that also includes impulsive control as represented by a proportional increase in the number of CTLs at some specific time points

$$\begin{aligned}
 \frac{dE_I}{dt} &= \frac{\beta V(N - E_I)}{\sigma + (N - E_I)} - \mu E_I - dE_I - aE_I Z, \\
 \frac{dE_T}{dt} &= \mu E_I + r\mu E_T - dE_T - aE_T Z, \\
 \frac{dV}{dt} &= kdE_I + kdE_T - d_v V, \\
 \frac{dL}{dt} &= \lambda + \frac{\eta E_T L}{\theta + V} - d_l L, \\
 \frac{dZ}{dt} &= s + \alpha ZL - d_z Z, \quad t \neq t_n, \\
 \Delta Z &= \omega Z, \quad t = t_n.
 \end{aligned}
 \tag{17}$$

Here,  $\Delta Z = Z(t_n^+) - Z(t_n^-)$ , where  $Z(t_n^-)$  and  $Z(t_n^+)$  represent the concentration of CTLs immediately before and after the impulse therapy, respectively. Smoothness properties of the right-hand sides of the original model (1) ensure global existence and uniqueness of the solution of the impulsive system<sup>62</sup>.

### Dynamics of impulsive system

In this section, we use one-dimensional impulsive differential equations to better understand the effects of impulse drug therapy. For this purpose, we consider an equation for CTLs from the system (17) and (18)

$$\begin{aligned}
 \frac{dZ}{dt} &= s + \alpha ZL - d_z Z, \quad \text{at } t \neq t_n, \\
 \Delta Z &= \omega Z, \quad \text{for } t = t_n, \quad n = 1, 2, 3, \dots
 \end{aligned}
 \tag{19}$$

We assume that during treatment, the number of HPV-specific CTLs increases by some constant proportion  $\omega$  (drug efficacy), where  $0 < \omega < 1$ .

Using relation (7), for maximal concentration of CTLs  $Z$ , we can rewrite that one-dimensional impulsive differential equation in the form

$$\begin{aligned} \frac{dZ}{dt} &= s - \zeta Z, \text{ for } t \neq t_n, \\ \Delta Z &= \omega Z, \text{ for } t = t_n \quad n = 1, 2, 3, \dots \end{aligned} \tag{20}$$

where  $\zeta = d_z - \alpha B_2 > 0$ , with  $B_2$  defined in (3). For single cycle  $t_n \leq t \leq t_{n+1}$  of impulsive treatment, the solution of the Eq. (19) is given by

$$Z(t_{n+1}^-) = \frac{s}{\zeta} \left[ 1 - e^{-\zeta(t_{n+1} - t_n)} \right] + Z(t_n^+) e^{-\zeta(t_{n+1} - t_n)}. \tag{21}$$

If we start in equilibrium state, the concentration of CTLs at the impulse times will satisfy

$$\begin{aligned} Z(t_1^-) &= \frac{s}{\zeta}, \\ Z(t_1^+) &= (1 + \omega) \frac{s}{\zeta}, \\ Z(t_2^-) &= (1 + \omega) \frac{s}{\zeta} e^{-\zeta(t_2 - t_1)} + \frac{s}{\zeta} \left[ 1 - e^{-\zeta(t_2 - t_1)} \right], \\ Z(t_2^+) &= (1 + \omega)^2 \frac{s}{\zeta} e^{-\zeta(t_2 - t_1)} + (1 + \omega) \frac{s}{\zeta} \left[ 1 - e^{-\zeta(t_2 - t_1)} \right], \\ Z(t_3^-) &= \frac{s}{\zeta} \left[ (1 + \omega)^2 e^{-\zeta(t_3 - t_1)} + (1 + \omega) e^{-\zeta(t_3 - t_2)} - (1 + \omega) e^{-\zeta(t_3 - t_1)} \right. \\ &\quad \left. + 1 - e^{-\zeta(t_3 - t_2)} \right], \\ Z(t_3^+) &= \frac{s}{\zeta} \left[ (1 + \omega)^3 e^{-\zeta(t_3 - t_1)} + (1 + \omega)^2 e^{-\zeta(t_3 - t_2)} - (1 + \omega)^2 e^{-\zeta(t_3 - t_1)} \right. \\ &\quad \left. + (1 + \omega) - (1 + \omega) e^{-\zeta(t_3 - t_2)} \right], \\ Z(t_4^-) &= \frac{s}{\zeta} \left[ (1 + \omega)^3 e^{-\zeta(t_4 - t_1)} + (1 + \omega)^2 e^{-\zeta(t_4 - t_2)} + (1 + \omega) e^{-\zeta(t_4 - t_3)} + \right. \\ &\quad \left. 1 - (1 + \omega)^2 e^{-\zeta(t_4 - t_1)} - (1 + \omega) e^{-\zeta(t_4 - t_2)} - e^{-\zeta(t_4 - t_3)} \right], \\ Z(t_4^+) &= \frac{s}{\zeta} \left[ (1 + \omega)^4 e^{-\zeta(t_4 - t_1)} + (1 + \omega)^3 e^{-\zeta(t_4 - t_2)} + (1 + \omega)^2 e^{-\zeta(t_4 - t_3)} + \right. \\ &\quad \left. (1 + \omega)^3 e^{-\zeta(t_4 - t_1)} - (1 + \omega)^2 e^{-\zeta(t_4 - t_2)} - (1 + \omega) e^{-\zeta(t_4 - t_3)} + (1 + \omega) \right], \end{aligned} \tag{22}$$

and so on. Hence, the general solution of impulsive system (20) can be found as

$$\begin{aligned} Z(t_n^-) &= \frac{s}{\zeta} \left[ (1 + \omega)^{(n-1)} e^{-\zeta(t_n - t_1)} + (1 + \omega)^{(n-2)} e^{-\zeta(t_n - t_2)} + \dots + (1 + \omega) e^{-\zeta(t_n - t_{n-1})} \right. \\ &\quad \left. + 1 - (1 + \omega)^{(n-2)} e^{-\zeta(t_n - t_1)} - (1 + \omega)^{(n-3)} e^{-\zeta(t_n - t_2)} - \dots - e^{-\zeta(t_n - t_{n-1})} \right], \end{aligned} \tag{23}$$

and

$$\begin{aligned} Z(t_n^+) &= \frac{s}{\zeta} \left[ (1 + \omega)^n e^{-\zeta(t_n - t_1)} + (1 + \omega)^{(n-1)} e^{-\zeta(t_n - t_2)} + \dots + (1 + \omega)^2 e^{-\zeta(t_n - t_{n-1})} \right. \\ &\quad \left. - (1 + \omega)^{(n-1)} e^{-\zeta(t_n - t_1)} - (1 + \omega)^{(n-2)} e^{-\zeta(t_n - t_2)} - \dots - (1 + \omega) e^{-\zeta(t_n - t_{n-1})} + (1 + \omega) \right] \end{aligned} \tag{24}$$

The above solutions given in (23) and (24) can help to predict the concentration of CTLs present just before and straight after the  $n^{\text{th}}$  number impulse.

For a fixed impulse interval, i.e. with  $t_{n+1} - t_n = \Upsilon$  being constant, we have

$$\begin{aligned} Z(t_n^-) &= \frac{s}{\zeta} \left[ 1 + (1 + \omega) e^{-\zeta \Upsilon} + (1 + \omega)^2 e^{-2\zeta \Upsilon} + \dots + (1 + \omega)^{n-1} e^{-(n-1)\zeta \Upsilon} \right. \\ &\quad \left. - e^{-\zeta \Upsilon} \left( 1 + (1 + \omega) e^{-\zeta \Upsilon} + \dots + (1 + \omega)^{n-2} e^{-(n-2)\zeta \Upsilon} \right) \right] \\ &= \frac{s}{\zeta} \left[ \frac{1 - (1 + \omega)^n e^{-n\zeta \Upsilon}}{1 - (1 + \omega) e^{-\zeta \Upsilon}} - e^{-\zeta \Upsilon} \frac{1 - (1 + \omega)^{n-1} e^{-(n-1)\zeta \Upsilon}}{1 - (1 + \omega) e^{-\zeta \Upsilon}} \right], \end{aligned}$$

and hence,

$$\lim_{n \rightarrow \infty} Z(t_n^-) = \frac{s}{\zeta} \left[ \frac{1}{1 - (1 + \omega)e^{-\zeta\Upsilon}} - e^{-\zeta\Upsilon} \frac{1}{1 - (1 + \omega)e^{-\zeta\Upsilon}} \right] = \frac{s}{\zeta} \left[ \frac{1 - e^{-\zeta\Upsilon}}{1 - (1 + \omega)e^{-\zeta\Upsilon}} \right]. \tag{25}$$

This is the maximum long-term concentration of CTLs just before impulsive therapy is applied. A similar expression can be obtained for the long-term maximum concentration of CTLs straight after the impulse therapy

$$\lim_{n \rightarrow \infty} Z(t_n^+) = (1 + \omega) \lim_{n \rightarrow \infty} Z(t_n^-) = \frac{s}{\zeta} \left[ \frac{(1 + \omega)(1 - e^{-\zeta\Upsilon})}{1 - (1 + \omega)e^{-\zeta\Upsilon}} \right]. \tag{26}$$

Suppose,  $Z_{min}$  is the minimum concentration of CTLs to gain disease-free periodic orbit. Then after the long-term therapy, to keep the concentration of CTLs at the level  $\tilde{Z}$  above this minimum level, we need to find the corresponding maximum time interval,  $\Upsilon_{max}$ , between two consecutive periods of therapy:

$$(1 + \omega) \frac{s}{\zeta} \left[ \frac{1 - e^{-\zeta\Upsilon_{max}}}{1 - (1 + \omega)e^{-\zeta\Upsilon_{max}}} \right] > Z_{min},$$

or,  $\Upsilon_{max} < \frac{1}{\zeta} \ln \left[ \frac{(Z_{min} - m)(1 + \omega)}{Z_{min} - m(1 + \omega)} \right]$ , where  $m = \frac{s}{\zeta}$ .

(27)

*Remark 1* It follows that, in the case of impulse drug dosing with fixed interval, we can derive a maximum length of interval of therapy using (27) that would keep the concentration of CTLs above the threshold  $Z_{min}$  of our choice. If we restrict  $\Upsilon < \Upsilon_{max}$ , then the concentration of CTL can be maintained above the threshold  $Z_{min}$  after long-term therapy.

### Existence and stability of disease-free periodic orbit

For a one-dimensional impulsive system

$$\frac{dZ(t)}{dt} = s - \zeta Z, \quad t \neq t_n, \quad \Delta Z = \omega Z. \tag{28}$$

we have the following Lemma from<sup>62–64</sup> that provides existence of a periodic solution

**Lemma 1** *The system given in (28) possesses a unique periodic solution denoted by  $\tilde{Z}(t)$  with period  $\Upsilon = t_{n+1} - t_n$  given by*

$$\tilde{Z}(t) = \frac{s}{\zeta} \left[ \frac{(1 + \omega)(1 - e^{-\zeta(t-t_n)})}{1 - (1 + \omega)e^{-\zeta\Upsilon}} \right], \quad t_n < t < t_{n+1}, \quad \tilde{Z}(0^+) = \frac{s}{\zeta} \left[ \frac{1 - e^{-\zeta\Upsilon}}{1 - (1 + \omega)e^{-\zeta\Upsilon}} \right]. \tag{29}$$

We now prove the following result regarding existence and stability of the disease-free periodic orbit in the system (17).

**Theorem 3** *The system (17) has a disease-free periodic orbit,  $\tilde{E}_0(0, 0, 0, \tilde{L}, \tilde{Z})$ , which is locally asymptotically stable if*

$$\tilde{\mathcal{R}}_0 = \frac{\beta kdN}{(N + \sigma)d_v} \int_0^\Upsilon \frac{(\mu + d + a\tilde{Z} - \mu r)dt}{(d + \mu + a\tilde{Z})(d + a\tilde{Z} - \mu r)} < 1.$$

*Proof* Let us denote the infection-free periodic orbit of the impulsive system (17) by  $\tilde{E}_0(0, 0, 0, \tilde{L}, \tilde{Z})$ , where

$$\tilde{Z}(t) = \frac{s}{\zeta} \left[ \frac{(1 + \omega)(1 - e^{-\zeta(t-t_n)})}{1 - (1 + \omega)e^{-\zeta\Upsilon}} \right], \quad t_n < t < t_{n+1},$$

with initial condition  $Z(0^+)$  as given in Lemma 1. To analyse stability of this periodic orbit, we compute the variational matrix at the periodic orbit  $\tilde{E}_0(0, 0, 0, \tilde{L}, \tilde{Z})$  as

$$M(t) = [\tilde{a}_{ij}]_{5 \times 5} = \begin{bmatrix} \tilde{a}_{11} & 0 & \frac{\beta N}{\sigma + N} & 0 & 0 \\ \mu & r\mu - d - a\tilde{Z} & 0 & 0 & 0 \\ kd & kd & -d_v & 0 & 0 \\ 0 & \frac{\eta \tilde{L}}{\theta} & 0 & -d_v & 0 \\ 0 & 0 & 0 & \alpha \tilde{Z} & \alpha \tilde{L} - d_z \end{bmatrix},$$

where  $\tilde{a}_{11} = -\mu - d - a\tilde{Z}$ . The variational matrix  $M$  gives the monodromy matrix  $\mathbb{P}$  as

$$\mathbb{P}(\Upsilon) = \mathbf{I}_4 \exp \left( \int_0^\Upsilon M(t) dt \right),$$

where  $\mathbf{I}_5$  is the  $5 \times 5$  identity matrix.

Let,  $\tilde{\rho}_i$ ,  $i = 1, 2, 3, 4, 5$  be the Floquet multipliers, and  $\mathbb{P}(\Upsilon) = \text{diag}(\tilde{\rho}_1, \tilde{\rho}_2, \tilde{\rho}_3, \tilde{\rho}_4, \tilde{\rho}_5)$ . We determine two of the multipliers as  $\tilde{\rho}_1 = \exp(-d_v \Upsilon)$ , and  $\tilde{\rho}_2 = \exp \left( \int_0^\Upsilon [\alpha \tilde{L} - d_z] dt \right)$ . Clearly,  $\tilde{\rho}_1 < 1$  is always true, and  $\tilde{\rho}_2 < 1$  holds when  $\alpha \tilde{L} - d_z < 0$  is satisfied. The remaining Floquet multipliers can be expressed as

$$\tilde{\rho}_i = \exp \left( \int_0^\Upsilon \xi_i dt \right), \quad i = 3, 4, 5,$$

where  $\xi_i$  are the roots of the cubic equation

$$\xi^3 + \tilde{\gamma}_1 \xi^2 + \tilde{\gamma}_2 \xi + \tilde{\gamma}_3 = 0, \tag{30}$$

with

$$\begin{aligned} \tilde{\gamma}_1 &= -(\tilde{a}_{11} + \tilde{a}_{22} + \tilde{a}_{33}), \quad \tilde{\gamma}_2 = \tilde{a}_{22}\tilde{a}_{33} + \tilde{a}_{11}\tilde{a}_{22} - \tilde{a}_{13}\tilde{a}_{31} + \tilde{a}_{11}\tilde{a}_{33}, \\ \tilde{\gamma}_3 &= -\tilde{a}_{13}\tilde{a}_{21}\tilde{a}_{31} + \tilde{a}_{13}\tilde{a}_{22}\tilde{a}_{31} - \tilde{a}_{11}\tilde{a}_{22}\tilde{a}_{33}. \end{aligned} \tag{31}$$

For the stability of the disease-free periodic orbit we need  $\tilde{\rho}_i < 1$ , which is true when real parts of  $\xi_i$  are negative. Using Routh–Hurwitz conditions, we find that the roots of Eq. (30) have negative real parts if

$$\tilde{\gamma}_1 > 0, \quad \tilde{\gamma}_3 > 0, \quad \text{and} \quad \tilde{\gamma}_1 \tilde{\gamma}_2 - \tilde{\gamma}_3 > 0. \tag{32}$$

Conditions in (32) are satisfied when  $\tilde{\mathcal{R}}_0 < 1$ , and in this case the Floquet multipliers  $\tilde{\rho}_i$  have the modulus less than unity. Thus, using Floquet theory, we conclude that the disease-free periodic orbit  $\tilde{E}_0(0, 0, 0, \tilde{L}, \tilde{Z})$  of the system (17) is asymptotically stable if  $\tilde{\mathcal{R}}_0 < 1$ .  $\square$

### Numerical bifurcation analyses and simulation

Using analytical findings from earlier sections, we now explore the dynamics of the models numerically, using baseline values of parameters as given in Table 1. Majority of parameter values in this Table follow earlier published work on similar models, and a few are estimated. Starting values of parameters were chosen with a view to agree with biological assumptions mentioned earlier.

Figure 2 illustrates how increasing the basic reproduction number  $\mathcal{R}_0$  results in the loss of stability of the disease-free steady state  $E_0$  when  $\mathcal{R}_0$  crosses the values of  $\mathcal{R}_0 = 1$ , at which point a stable chronic steady state  $E^*$  appears.

In Fig. 3 we show how stability of the DFE  $E_0$  changes with parameters. As expected, the DFE  $E_0$  is stable for lower values of the disease transmission rate  $\beta$ , and it also stabilises with increased rate of production of Langerhans cells  $\lambda$ , increased rate of production of CTLs  $s$ , or with a higher rate  $a$ , at which CTLs destroy infected cells.

In Fig. 4, we demonstrate temporal behavior of all cell populations of the system. Starting a small number of infected cells, the population of susceptible cells, as represented by  $[N - E_I(t) - E_T(t)]$ , decreases, as

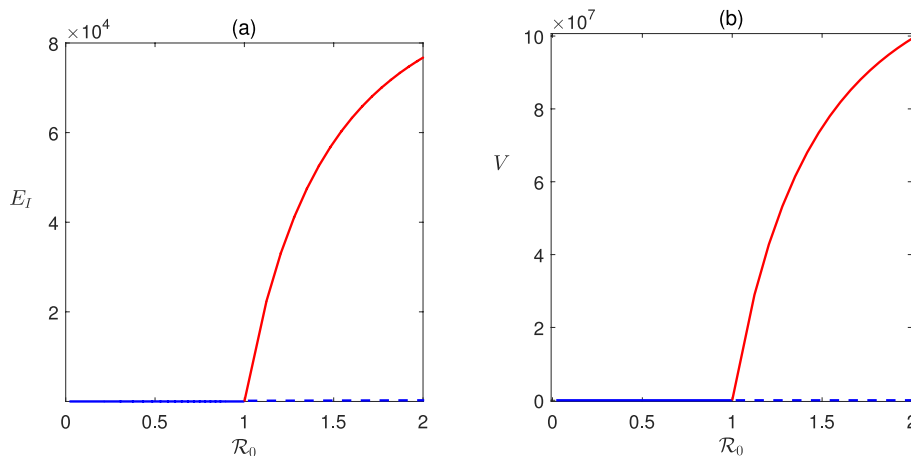


**Fig. 2.** Bifurcation diagram of the model (1). The disease-free steady state  $E_0$ , shown in blue, is stable for  $\mathcal{R}_0 < 1$  and unstable for  $\mathcal{R}_0 > 1$ , where the chronic equilibrium  $E^*$  exists and is stable.

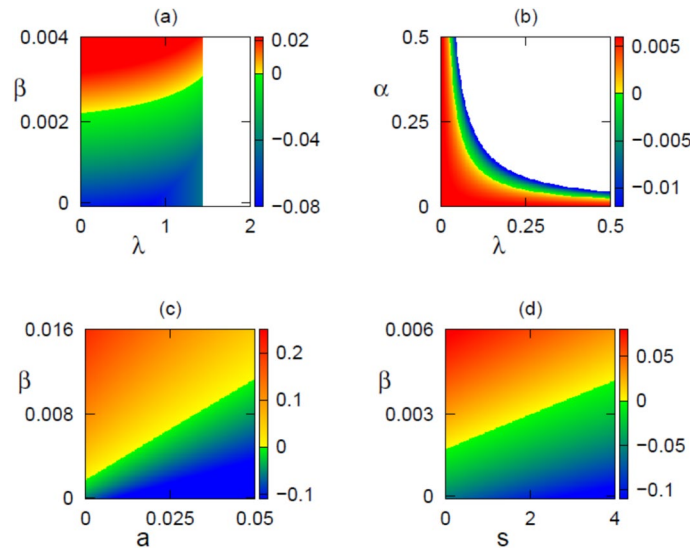


**Fig. 3.** Stability of the disease-free equilibrium  $E_0$  for parameter values from Table 1. Color code represents the maximum real part of characteristic eigenvalues of the DFE. White region indicates an area, where there are no feasible equilibria.

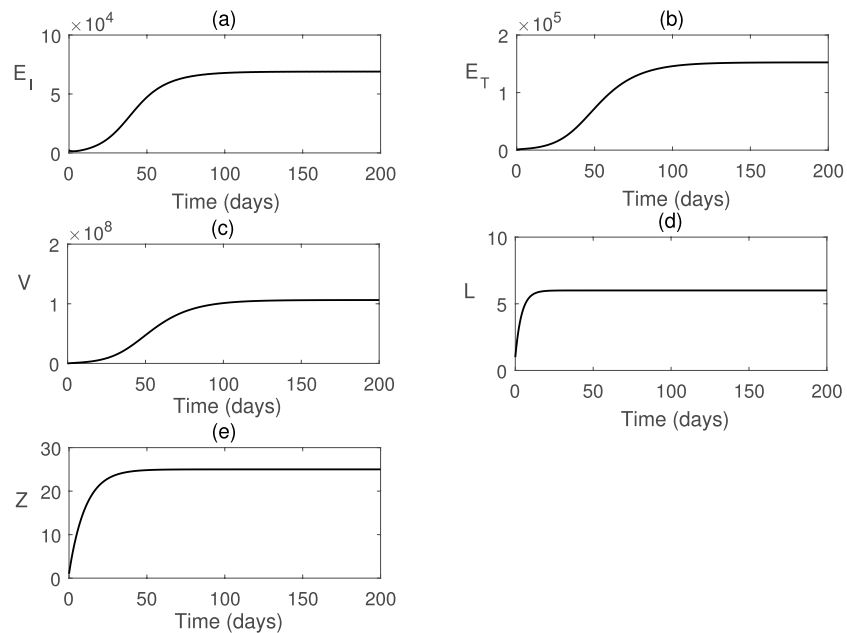


**Fig. 4.** Temporal solution of the system (1) with parameter values from Table 1.

infection progresses, and some portion of this population moves to the infected class. We observe that at an early stage the growth of infection is slow, but then it increases, until eventually it saturates, with the system settling on a stable steady state  $E^*$ , which represents a chronic infection. This could be attributed to either a failure of the immune system, or to an immune evasion strategy pursued by HPV. Figure 5 illustrates global stability of chronic equilibrium, with trajectories starting at different initial conditions, but eventually converging on the stable chronic steady state  $E^*$ .

In Fig. 6 we have plotted the numerical solutions of impulsive system (17) and (18) for two different impulse intervals,  $\Upsilon = 7$  days and  $\Upsilon = 14$  days, under assumption that at each application of therapy, the concentration of CTLs increases by  $\omega = 0.05$  of its current value. The infection is cleared more rapidly when the interval of dosing therapy is lower ( $\Upsilon = 7$  days). In Fig. 7 we plot a similar result for a fixed impulse interval of 14 days, but with two different values of  $\omega$  that quantifies the increase in CTLs after each therapy. Increasing drug efficacy or dose, which corresponds to a higher value of  $\omega$  results in lower peak number of infected cells and faster clearance of infection.

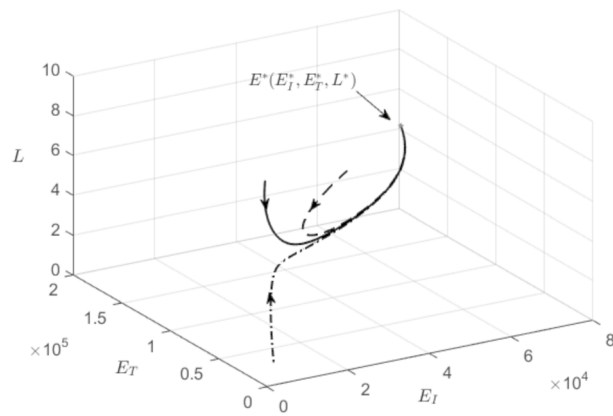


**Fig. 5.** Phase space of the system (1) for three different initial conditions with parameter values from Table 1. In this parameter regime, the chronic steady state  $E^*$  is stable, and all trajectories eventually approach this state.

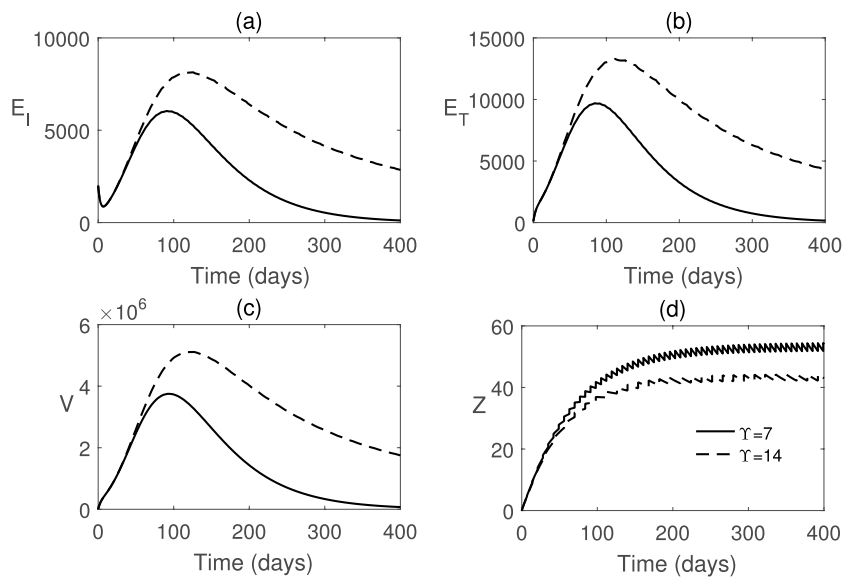


**Fig. 6.** Temporal dynamics of the model (17) and (18) with impulsive immune therapy for a fixed interval of  $\Upsilon = 7$  days (solid line) and  $\Upsilon = 14$  days (dashed line). The values of other parameter are given in Table 1.

Finally, Fig. 8 presents temporal dynamics of sensitivity functions for the viral population  $V(t)$  depending on different parameters. One can note that at the initial stages of infection, viral population is most sensitive positively to the increase in the infection rate  $\beta$  and negatively to the increase in the rate of death of infected cells  $\mu$ . Sensitivity with respect to parameters  $\lambda$  and  $s$  that control constant growth in the number of Langerhans cells and HPV-specific CTLs, respectively, is negative and monotonic. The only other positive sensitivity function for viral population is associated with parameter  $k$  that characterizes the burst size, thus controlling how many new infections can arise from a single infected cell upon its death.

## Discussion and conclusion

In this paper, we have studied a mathematical model of within-host HPV dynamics that includes two populations of infected cells, expressing lower and higher amounts of E6/E7 oncogenes, the Langerhans cells and HPV-specific CTLs. Both LCs and CTLs play important role in orchestrating immune response against the HPV through recognizing and destroying infected cells. We have shown well-posedness of our model in terms of non-negativity and boundedness of its solutions. To characterize the onset of chronic infection and obtain conditions for disease elimination, we have derived a basic reproduction number using the next generation matrix approach. We performed numerical bifurcation analyses and simulations to explore how the dynamics and stability of the steady states changes with system parameters. These results show that increasing the values of parameters, characterizing immune response, leads to stabilization of the disease-free equilibrium. In contrast, increasing disease transmission rate results in the establishment of the globally stable chronic steady state. We

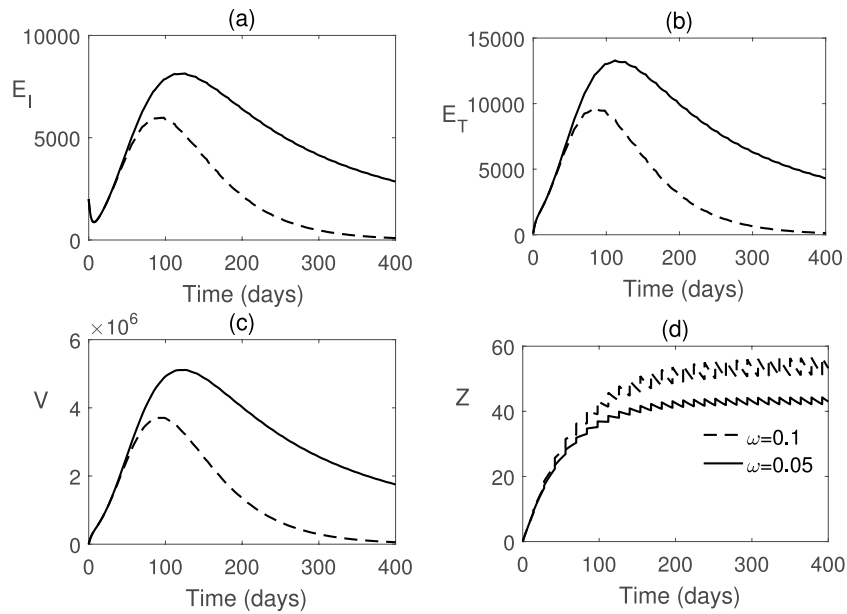


**Fig. 7.** Impulsive application of immune therapy as described by the model (17) and (18) with  $\omega = 0.05$ ( solid line) and  $\omega = 0.1$ ( dashed line) taking a fixed interval  $\Upsilon = 14$  days. The values of other parameter are given in Table 1.

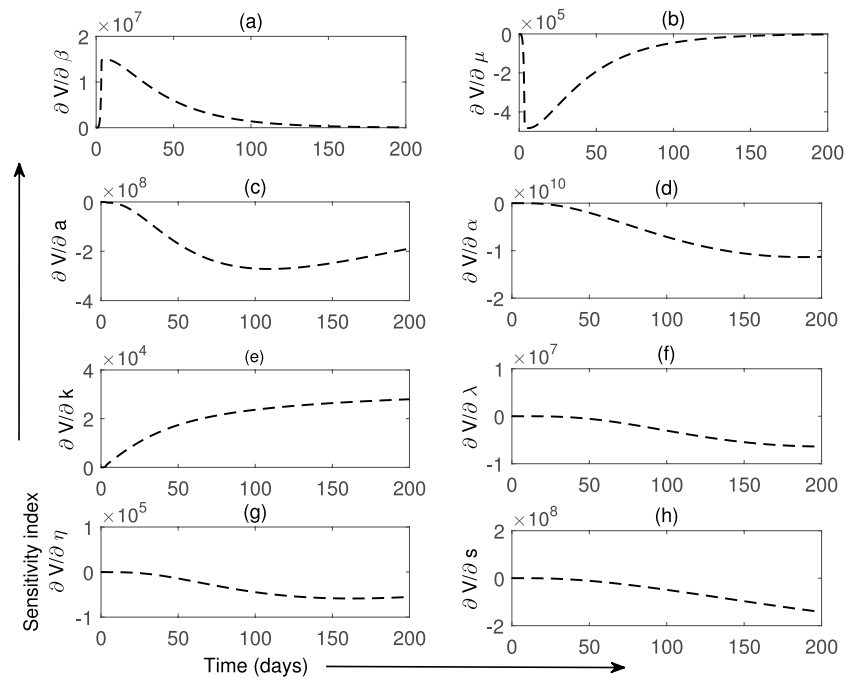


**Fig. 8.** Sensitivity of viral population to changes in model parameters as a function of time,  $t$ .

have also analyzed the dynamics of impulsive therapy for the treatment of HPV infection under different therapy regimes.

The results of this study results may be helpful for better understanding of the complexity of immune response to HPV and the development of HPV-related cancers. In particular, they show an intricate interplay between Langerhans cells and HPV-specific CTLs that is required for clearing the infection. This is particularly important in light of the immune evasion strategy employed by the HPV, which is able to inhibit interferons, minimize antigen production, and indirectly reduce the capacity of LCs to stimulate CTLs.

There are several directions, in which the work presented in this paper can be expanded. In our model, we made a simplifying assumption that both types of infected cells produce virions at exactly the same rate. This

assumption can be removed to allow different rates of virion production, which may better reflect the reality due to different types of infected cells expressing significantly different concentrations of oncogenes. Similarly, CTLs were assumed to destroy infected cells at the same rate, but since these are antigen-specific CTLs, the model can consider these rates to be different, to correspond to levels of expression of oncoproteins. Another avenue to explore is to represent dynamics of the virus and the immune responses using fractional derivatives, as has recently been done for some other viral diseases<sup>65–67</sup>.

## Data availability

The data sets used and/or analysed during the current study are available from the corresponding author on reasonable request.

Received: 14 November 2024; Accepted: 14 May 2025

Published online: 20 May 2025

## References

- Arbyn, M. et al. Estimates of incidence and mortality of cervical cancer in 2018: A worldwide analysis. *Lancet Glob. Health* **8**, e191–e203 (2020).
- World Health Organization, et al. World cancer report, chapter 5.12. *Regional Office for South-East Asia* **630** (2014).
- World Health Organization, et al. World cancer report 2014. 2014: Chapter 1.1.
- World Health Organization. Global strategy to accelerate the elimination of cervical cancer as a public health problem (2020).
- Stanley, M. Immunobiology of HPV and HPV vaccines. *Gynecol. Oncol.* **109**, S15–S21 (2008).
- Garces, A. H. I. et al. Approach and management of cervical cancer. *International Manual of Oncology Practice: iMOP-Principles of Oncology* 491–549 (2019).
- Yoshinouchi, M. et al. Analysis by multiplex PCR of the physical status of human papillomavirus type 16 DNA in cervical cancers. *J. Clin. Microbiol.* **37**, 3514–3517 (1999).
- Syrjänen, S. M. & Syrjänen, K. J. New concepts on the role of human papillomavirus in cell cycle regulation. *Ann. Med.* **31**, 175–187 (1999).
- Thomas, M., Pim, D. & Banks, L. The role of the E6–p53 interaction in the molecular pathogenesis of HPV. *Oncogene* **18**, 7690 (1999).
- Park, T.-W., Fujiwara, H. & Wright, T. C. Molecular biology of cervical cancer and its precursors. *Cancer* **76**, 1902–1913 (1995).
- Holowaty, P., Miller, A. B., Rohan, T. & To, T. Natural history of dysplasia of the uterine cervix. *J. Natl Cancer Inst.* **91**, 252–258 (1999).
- Zur Hausen, H. Papillomavirus infections—a major cause of human cancers. *Biochim. Biophys. Acta BBA Rev. Cancer* **1288**, F55–F78 (1996).
- Murphy, K. & Weaver, C. *Janeway's Immunobiology* (Garland Science, 2017).
- Renoux, V. M. et al. Human papillomavirus entry into NK cells requires CD16 expression and triggers cytotoxic activity and cytokine secretion. *Eur. J. Immunol.* **41**, 3240–3252 (2011).
- Romani, N. et al. Presentation of exogenous protein antigens by dendritic cells to T cell clones. Intact protein is presented best by immature, epidermal langerhans cells. *J. Exp. Med.* **169**, 1169–1178 (1989).
- Stingl, G., Katz, S. I., Clement, L., Green, I. & Shevach, E. M. Immunologic functions of Ia-bearing epidermal Langerhans cells. *J. Immunol.* **121**, 2005–2013 (1978).
- Stanley, M. Immune responses to human papillomavirus. *Vaccine* **24**(suppl. 1), S16–S22 (2006).
- Sasagawa, T., Takagi, H. & Makinoda, S. Immune responses against human papillomavirus (HPV) infection and evasion of host defense in cervical cancer. *J. Infect. Chemother.* **18**, 807–815 (2012).
- Kirschner, D. & Panetta, J. C. Modeling immunotherapy of the tumor-immune interaction. *J. Math. Biol.* **37**, 235–252 (1998).
- de Boer, R. J. & Hogeweg, P. Interactions between macrophages and T-lymphocytes: Tumor sneaking through intrinsic to helper T cell dynamics. *J. Theor. Biol.* **120**, 331–351 (1986).
- Kuznetsov, V. & Makalkin, I. Bifurcation analysis of a mathematical model of the interaction of cytotoxic lymphocytes with tumor cells. The effect of immunologic amplification of tumor growth and its interconnection with other “anomalous” phenomena of oncoimmunology. *Biofizika* **37**, 1063–1070 (1992).
- Kuznetsov, V. A., Makalkin, I. A., Taylor, M. A. & Perelson, A. S. Nonlinear dynamics of immunogenic tumors: Parameter estimation and global bifurcation analysis. *Bull. Math. Biol.* **56**, 295–321 (1994).
- Dingli, D. & Michor, F. Successful therapy must eradicate cancer stem cells. *Stem Cells* **24**, 2603–2610 (2006).
- Belostotski, G. & Freedman, H. A control theory model for cancer treatment by radiotherapy. *International Journal of Pure and Applied Mathematics* **25** (2004).
- Freedman, H. & Belostotski, G. Perturbed models for cancer treatment by radiotherapy. *Differ. Equ. Dyn. Syst.* **17**, 115–133 (2009).
- Liu, Z., Zhong, S., Yin, C. & Chen, W. Permanence, extinction and periodic solutions in a mathematical model of cell populations affected by periodic radiation. *Appl. Math. Lett.* **24**, 1745–1750 (2011).
- Isaeva, O. & Osipov, V. Different strategies for cancer treatment: Mathematical modelling. *Comput. Math. Methods Med.* **10**, 253–272 (2009).
- Rajan, P. K., Kuppusamy, M. & Egbelowo, O. F. A mathematical model for human papillomavirus and its impact on cervical cancer in India. *J. Appl. Math. Comput.* **69**, 753–770 (2023).
- Murall, C. L., Bauch, C. T. & Day, T. Could the human papillomavirus vaccines drive virulence evolution?. *Proc. R. Soc. B* **282**, 20141069 (2015).
- Verma, M. et al. Modeling the mechanisms by which HIV-associated immunosuppression influences HPV persistence at the oral mucosa. *PLoS ONE* **12**, e0168133 (2017).
- Doorbar, J. Molecular biology of human papillomavirus infection and cervical cancer. *Clin. Sci.* **100**, 525–541 (2006).
- Murall, C., McCann, K. & Bauch, C. Revising ecological assumptions about Human papillomavirus interactions and type replacement. *J. Theor. Biol.* **350**, 98–109 (2014).
- Moscicki, A.-B., Schiffman, M., Kjaer, S. & Villa, L. Chapter 5: Updating the natural history of HPV and anogenital cancer. *Vaccine* **24**(suppl. 3), 42–51 (2006).
- Leong, C. M., Doorbar, J., Nindl, I., Yoon, H. & Hibma, M. H. Loss of epidermal langerhans cells occurs in human papillomavirus alpha, gamma, and mu but not beta genus infections. *J. Investig. Dermatol.* **130**, 472–480 (2010).
- Parr, M. B. & Parr, E. L. Langerhans cells and T lymphocyte subsets in the murine vagina and cervix. *Biol. Reprod.* **44**, 491–498 (1991).
- Caberg, J. et al. Increased migration of Langerhans cells in response to HPV16 E6 and E7 oncogene silencing: Role of CCL20. *Cancer Immunol. Immunother.* **58**, 39–47 (2009).

37. Dai, W., Gui, L., Du, H., Li, S. & Wu, R. The association of cervicovaginal Langerhans cells with clearance of human papillomavirus. *Front. Immunol.* **13**, 918190 (2022).
38. Guess, J. & McCance, D. Decreased migration of Langerhans precursor-like cells in response to human keratinocytes expressing human papillomavirus type 16 E6/E7 is related to reduced macrophage inflammatory protein-3 $\alpha$  production. *J. Virol.* **79**, 14852–14862 (2005).
39. D'Costa, Z. et al. Transcriptional repression of E-Cadherin by human papillomavirus type 16 E6. *PLoS ONE* **7**, e48954 (2012).
40. Hatano, T., Sano, D., Takahashi, H. & Oridate, N. Pathogenic role of immune evasion and integration of human papillomavirus in oropharyngeal cancer. *Microorganisms* **9**, 891 (2021).
41. Coddington, E. A. & Levinson, N. *Theory of Ordinary Differential Equations* (McGraw-Hill, 1955).
42. Chicone, C. *Ordinary Differential Equations with Applications* (Springer, 2006).
43. Brauer, F. & Castillo-Chavez, C. *Mathematical Models in Population Biology and Epidemiology* (Springer, 2010).
44. Diekmann, O. & Heesterbeek, J. A. P. *Mathematical Epidemiology of Infectious Diseases: Model Building, Analysis and Interpretation* (Wiley, 2000).
45. Keeling, M. J. & Rohani, P. *Modeling Infectious Diseases in Humans and Animals* (Princeton University Press, 2008).
46. Yang, H. & Wie, J. Analyzing global stability of a viral model with general incidence rate and cytotoxic T lymphocytes immune response. *Nonlinear Dyn.* **85**, 713–722 (2015).
47. Ghosh, I. Within host dynamics of sars-cov-2 in humans: Modeling immune responses and antiviral treatments. *SN Comput. Sci.* **2**, 482 (2021).
48. Aavani, P. & Allen, L. J. S. The role of CD4 T cells in immune system activation and viral reproduction in a simple model for HIV infection. *Appl. Math. Model.* **75**, 210–222 (2019).
49. Williams, B. et al. The reproduction number and its probability distribution for stochastic viral dynamics. *J. R. Soc. Interface* **21**, 20230400 (2024).
50. Diekmann, O., Heesterbeek, J. A. P. & Metz, J. A. On the definition and the computation of the basic reproduction ratio  $r_0$  in models for infectious diseases in heterogeneous populations. *J. Math. Biol.* **28**, 365–382 (1990).
51. Van den Driessche, P. & Watmough, J. Reproduction numbers and sub-threshold endemic equilibria for compartmental models of disease transmission. *Math. Biosci.* **180**, 29–48 (2002).
52. Rihan, F. A. Sensitivity analysis for dynamic systems with time-lags. *J. Comput. Appl. Math.* **151**, 445–462 (2003).
53. Ribeiro, R. M., Mohri, H., Ho, D. D. & Perelson, A. S. In vivo dynamics of T cell activation, proliferation, and death in HIV-1 infection: Why are CD4+ but not CD8+ T cells depleted? *Proc. Natl. Acad. Sci.* **99**, 15572–15577 (2002).
54. Asquith, B., Edwards, C. T., Lipsitch, M. & McLean, A. R. Inefficient cytotoxic T lymphocyte-mediated killing of HIV-1-infected cells in vivo. *PLoS Biol.* **4**, e90 (2006).
55. Culp, T. D. & Christensen, N. D. Kinetics of in vitro adsorption and entry of papillomavirus virions. *Virology* **319**, 152–161 (2004).
56. De Paepe, M. & Taddei, F. Viruses' life history: Towards a mechanistic basis of a trade-off between survival and reproduction among phages. *PLoS Biol.* **4**, e193 (2006).
57. Su, J.-H. et al. Immunotherapy for cervical cancer: Research status and clinical potential. *BioDrugs* **24**, 109–129 (2010).
58. Yan, F., Cowell, L., Tomkies, A. & Day, A. Therapeutic vaccination for HPV-mediated cancers. *Curr. Otorhinolaryngol. Rep.* **11**, 44–61 (2023).
59. Shamseddine, A., Burman, B., Lee, N., Zamarin, D. & Riaz, N. Tumor immunity and immunotherapy for HPV-related cancers. *Cancer Discov.* **11**, 1896–1912 (2021).
60. Stevanović, S. et al. Complete regression of metastatic cervical cancer after treatment with human papillomavirus-targeted tumor-infiltrating T cells. *J. Clin. Oncol.* **33**, 1543–1550 (2015).
61. Stevanović, S. et al. Advancing immunotherapies for HPV-related cancers: Exploring novel vaccine strategies and the influence of tumor microenvironment. *Vaccines* **11**, 1354 (2023).
62. Lakshmikantham, V. et al. *Theory of Impulsive Differential Equations* Vol. 6 (World scientific, 1989).
63. Basir, F. A., Venturino, E. & Roy, P. K. Effects of awareness program for controlling mosaic disease in *Jatropha curcas* plantations. *Math. Methods Appl. Sci.* **40**, 2441–2453 (2017).
64. Chatterjee, A. N., Al Basir, F. & Takeuchi, Y. Effect of DAA therapy in hepatitis C treatment—An impulsive control approach. *Math. Biosci. Eng.* **18**, 1450–1464 (2021).
65. Fantaye, A. & Birhanu, Z. Modeling and analysis for the transmission dynamics of cotton leaf curl virus using fractional order derivatives. *Heliyon* **9**, e16877 (2023).
66. Fantaye, A. Fractional order for the transmission dynamics of coffee berry diseases (CBD). *Eur. J. Appl. Math.* <https://doi.org/10.1017/S0956792524000780> (2024).
67. Din, A., Li, Y., Khan, F. M., Khan, Z. U. & Liu, P. On analysis of fractional order mathematical model of hepatitis B using Atangana-Baleanu Caputo (ABC) derivative. *Fractals* **30**, 2240017 (2022).

## Acknowledgements

We would like to thank the editor as well as the referees for their valuable insight, which has significantly let improvements in our work. The authors extend their appreciation to the Deanship of Research and Graduate studies at King Khalid University grant number RGP2/58/46. Also the authors acknowledge the UAE University for funding this work.

## Declarations

## Competing interest

The authors declare no conflict of interest.

## Additional information

**Correspondence** and requests for materials should be addressed to H.J.A.

**Reprints and permissions information** is available at [www.nature.com/reprints](http://www.nature.com/reprints).

**Publisher's note** Springer Nature remains neutral with regard to jurisdictional claims in published maps and institutional affiliations.

**Open Access** This article is licensed under a Creative Commons Attribution-NonCommercial-NoDerivatives 4.0 International License, which permits any non-commercial use, sharing, distribution and reproduction in any medium or format, as long as you give appropriate credit to the original author(s) and the source, provide a link to the Creative Commons licence, and indicate if you modified the licensed material. You do not have permission under this licence to share adapted material derived from this article or parts of it. The images or other third party material in this article are included in the article's Creative Commons licence, unless indicated otherwise in a credit line to the material. If material is not included in the article's Creative Commons licence and your intended use is not permitted by statutory regulation or exceeds the permitted use, you will need to obtain permission directly from the copyright holder. To view a copy of this licence, visit <http://creativecommons.org/licenses/by-nc-nd/4.0/>.

© The Author(s) 2025